Mechanisms for generating toroidal rotation in tokamaks without external momentum input[a)]

W. M. Solomon,[1,b)] K. H. Burrell,[2] A. M. Garofalo,[2] S. M. Kaye,[1] R. E. Bell,[1] A. J. Cole,[3] J. S. deGrassie,[2] P. H. Diamond,[4] T. S. Hahm,[1] G. L. Jackson,[2] M. J. Lanctot,[5] C. C. Petty,[2] H. Reimerdes,[5] S. A. Sabbagh,[5] E. J. Strait,[2] T. Tala,[6] and R. E. Waltz[2]
[1]*Princeton Plasma Physics Laboratory, Princeton University, Princeton, New Jersey 08543, USA*
[2]*General Atomics, P.O. Box 85608, San Diego, California 92186-5608, USA*
[3]*University of Wisconsin, Madison, Wisconsin 53706-1609, USA*
[4]*Center for Astrophysics and Space Sciences, University of California, San Diego, 9500 Gilman Drive, La Jolla, California 92093-0424, USA*
[5]*Columbia University, New York, New York 10027, USA*
[6]*Association EURATOM-Tekes, VTT, P.O. Box 1000, FIN-02044 VTT, Finland*

(Received 2 December 2009; accepted 2 February 2010; published online 30 March 2010)

Recent experiments on DIII-D [J. L. Luxon, Nucl. Fusion **42**, 614 (2002)] and National Spherical Torus Experiment (NSTX) [M. Ono *et al.*, Nucl. Fusion **40**, 557 (2000)] have focused on investigating mechanisms of driving rotation in fusion plasmas. The so-called intrinsic rotation is generated by an effective torque, driven by residual stresses in the plasma, which appears to originate in the plasma edge. A clear scaling of this intrinsic drive with the H-mode pressure gradient is observed. Coupled with the experimentally inferred pinch of angular momentum, such an edge source is capable of producing sheared rotation profiles. Intrinsic drive is also possible directly in the core, although the physics mechanisms are much more complex. Another option which is being explored is the use of nonresonant magnetic fields for spinning the plasma. It is found beneficially that the torque from these fields can be enhanced at low rotation, which assists in spinning the plasma from rest, and offers increased resistance against plasma slowing. © *2010 American Institute of Physics*. [doi:10.1063/1.3328521]

I. INTRODUCTION

Rotation in tokamaks is generally considered beneficial to fusion plasmas, both through improvements in stability[1] and confinement.[2] The optimum rotation profile for future devices such as ITER (Ref. 3) is still an active area of research, but the need for rotation profile control is clearly of value. In present day devices, rotation is most commonly driven by external means through the use of neutral beams. However, in future burning plasmas, the torque capable of being driven by beams is expected to be small. Hence, alternative means of achieving rotation in tokamaks are being investigated.

The angular momentum balance equation describes how toroidal rotation is driven and damped from the plasma, which we may write in a simplified form as

$$mnR\frac{\partial V_\phi}{\partial t} = \Sigma\,\eta - \nabla\cdot\Pi_\phi - \frac{mnRV_\phi}{\tau_{\rm damp}}, \tag{1}$$

where V_ϕ is the toroidal velocity, η is any local torque density (such as provided by beams), Π_ϕ is the toroidal momentum flux arising, for example, from classical, neoclassical, and turbulent Reynolds stress (so generally considered the transport term), $\tau_{\rm damp}$ is an effective damping time associated with drag on the plasma, such as due to nonresonant magnetic fields (NRMFs), and other variables are of standard usage. Additional terms may also be considered; a more complete description of such terms can be found in Ref. 4. In principle, one can consider all terms other than the direct torque as possible drivers of rotation. As such, this paper will focus on exploiting the terms associated with transport and NRMF damping as a means of generating and controlling plasma rotation.

The momentum transport term is most commonly considered diffusive in nature, i.e., $\Pi_\phi = -mnR\chi_\phi^{\rm eff}\partial V_\phi/\partial r$, where $\chi_\phi^{\rm eff}$ is an effective momentum diffusivity. However, it has been recognized that such a simple model is inadequate to describe the observed momentum transport. A more complete representation of the transport induced momentum flux can be written as

$$\Pi_\phi = -mnR\left(\chi_\phi\frac{\partial V_\phi}{\partial r} - V_{\rm pinch}V_\phi\right) + \Pi_{\rm RS}, \tag{2}$$

where $V_{\rm pinch}$ is the angular momentum pinch velocity and $\Pi_{\rm RS}$ is the flux due to the so-called "residual stress." Note that while an equivalent pinch term exists in the particle balance equation, there is no such counterpart for the residual stress term.

All mechanisms contributing to toroidal angular momentum (TAM) flow involve breaking the intrinsic symmetry of the toroidal gyrokinetic equation under reversal of the parallel velocity ($v_\parallel \to -v_\parallel$) with simultaneous reversal of the poloidal angle ($\theta \to -\theta$) [or equivalently radial distance from a singular surface ($x \to -x$)]. Specifically, the Kelvin–Helmholtz drive (normally associated with simple diffusion

[a)]Paper NI3 2, Bull. Am. Phys. Soc. **54**, 181 (2009).
[b)]Invited speaker. Electronic mail: wsolomon@pppl.gov.

χ_ϕ) and the toroidal Coriolis force [associated with V_{pinch} (Refs. 5 and 6)] result from breaking $v_\parallel \rightarrow -v_\parallel$, and the residual stress breaks radial symmetry $x \rightarrow -x$ (or $\theta \rightarrow -\theta$). Various mechanisms have been discussed theoretically leading to residual stress generation, including $E \times B$ shear[7,8] ($x \rightarrow -x$), geometrical up-down asymmetries[9] ($\theta \rightarrow -\theta$), and charge separation from the polarization drift.[10] It should be noted that Π_{RS} can have either sign, depending, for example, on the sign of the $E \times B$ shear.[11] These mechanisms of TAM flow were recently illustrated in local flux-tube gyrokinetic simulations[11] with the GYRO code.[12] A pinch of angular momentum has recently been investigated experimentally[13–15] as have nondiffusive, nonpinch terms.[16–18]

Experimentally, the application of NRMFs has been shown to apply a torque on the plasma.[19–21] Theoretically, this can be understood in terms of increased radial neoclassical transport resulting from nonuniformity of the magnetic field caused by the nonaxisymmetric fields (i.e., broken toroidal symmetry).[4,22–24] The radial transport associated with these fields is responsible for the toroidal torque being exerted on the plasma. Although NRMFs act as a drag on the plasma rotation [as represented by the third term on the right hand side of Eq. (1)], the process is such that it drags the rotation to a finite rotation state,[4,24] i.e.,

$$\eta_{\text{NRMF}} \sim -k(V_\phi - V_\phi^*), \tag{3}$$

where k can be considered a "strength" coefficient to the torque, which depends on parameters such as the size of the magnetic field perturbation, density, and temperature among others. This "offset" rotation is in the direction counter to the plasma current and has recently been observed experimentally.[21]

II. INTRINSIC ROTATION GENERATION

A considerable amount of work has focused on trying to characterize the intrinsic rotation for projection to future devices such as ITER.[25] Although this is a critical first step, it does not address the underlying physics responsible for the drive of this rotation. While it is evident that a residual stresslike term must be responsible for the initial spin-up, we cannot readily measure it under "intrinsic conditions," where there is finite rotation. That is because when the velocity remains finite, all three terms in Eq. (2) are active, making it more challenging to directly estimate the contribution of Π_{RS}. A better approach is therefore to use external means to null out the plasma rotation. If this is achieved, then the velocity and its gradient is zero, and we are left with only the residual stress term.

Previous work[17] on DIII-D (Ref. 26) has indeed demonstrated that a finite external torque, in that case provided by neutral beams, is required to null out the intrinsic rotation. With the rotation effectively held at zero under steady conditions across the plasma profile, the effective intrinsic torque associated with the residual stress can be inferred as approximately the negative of the externally applied neutral beam torque, i.e., $\eta_{\text{intrinsic}} = -\nabla \cdot \Pi_{\text{RS}} = -\eta_{\text{NBI}}$. In that particular case, it was found that the intrinsic torque was in the cocurrent direction and equivalent to approximately one neutral beam source.

Of course, even though the rotation is very small across the profile compared with typical DIII-D rotation profiles from coinjected neutral beam injection (NBI), in reality, the measured rotation profile is not identically zero everywhere. However, we can estimate the potential for the small remaining rotation to contribute momentum flux. Assuming momentum diffusivities typical for DIII-D plasmas, one computes a value of order 0.1 Nm, more than an order of magnitude below the intrinsic torque values we typically observe. An additional complication comes from the fact that we measure the carbon impurity rotation as opposed to the main ion (deuterium) rotation. However, neoclassically, the large intrinsic torque cannot be a consequence of this measurement difference; in fact, the neoclassically predicted deuterium rotation tends to be shifted towards the cocurrent direction relative to the carbon impurity, if anything resulting in our intrinsic torque measurement being an *underestimate*.

While nulling out the plasma rotation provides the clearest method of measuring the residual stress driven torque, it is also relatively time consuming to make this measurement in steady state. By relaxing the steady state requirement, one can more efficiently acquire data related to the intrinsic torque. To the extent that one can at least drive the rotation profile to zero *transiently*, again by external means such as NBI, one can still eliminate the standard transport terms arising from diffusion and the pinch, and determine the intrinsic torque density as

$$\eta_{\text{intrinsic}} = -\eta_{\text{NBI}} + mnR\,\partial V_\phi/\partial t, \tag{4}$$

where a correction term must be added to account for the fact that the angular momentum is evolving. Depending on how slowly the external neutral beam torque is ramped, this correction can be relatively minor. An example of this is shown in Fig. 1. In this analysis, the neutral beam torque is computed within TRANSP (Ref. 27) using the NUBEAM package.[28,29] This calculation includes classical fast ion transport and accounts for losses associated with shine through and direct orbit loss. For the plasma shown in Fig. 1, such losses are not insignificant (200 and 800 kW, respectively, from a total injected power of 6.7 MW).

As was noted in Ref. 17, nonclassical fast ion transport, which is for example associated with Alfvén eigenmode instabilities, can quantitatively alter the calculated neutral beam torque profile, and with it, the inferred intrinsic torque. Even in these cases, however, the qualitative interpretation of the intrinsic torque is not dramatically altered, although the details clearly can be. To minimize these complications, the plasmas discussed in this paper were chosen because of the low (undetectable) level of Alfvén eigenmode activity and because the calculated neutron rates were within error bars of the measured neutron rates. Under these conditions, the neutral beam model used within TRANSP is believed to be reliable.

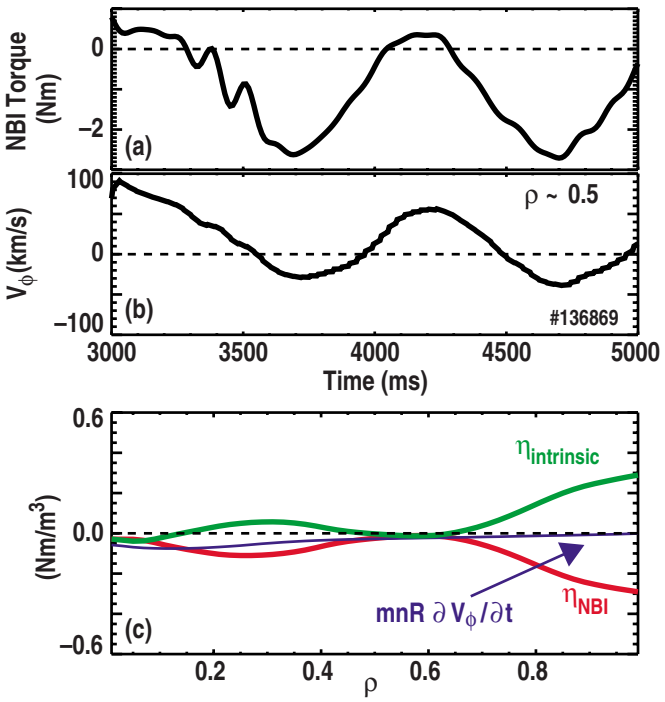

FIG. 1. (Color online) (a) Neutral beam torque and (b) midradius toroidal velocity during a preprogrammed NBI torque ramp at constant power on DIII-D. (c) Determination of intrinsic torque profile correcting for the transient rotation behavior following Eq. (4).

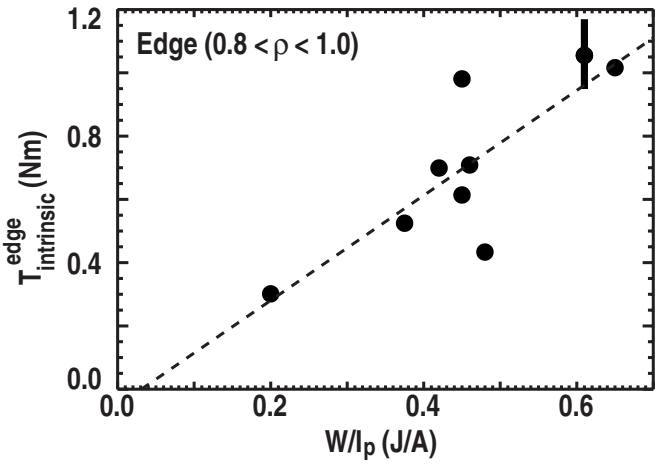

FIG. 2. Plot of edge intrinsic torque (integrated between $0.8<\rho<1.0$) and the global quantity W/I_p from a sequence of DIII-D H-mode plasmas. A typical error bar for this measurement is indicated and a linear regression fit to the data set is overplotted.

A. Effective drive of intrinsic rotation in the plasma edge

A cross-machine database on intrinsic rotation has been established.[25] Various regressions have been performed to try to capture some kind of intrinsic rotation scaling; however, the simplest version of these has indicated a scaling as the ratio of the stored energy to the plasma current, W/I_p. While such an empirical scaling based on global quantities does not offer any detailed insight into the generation of the intrinsic rotation, it does nonetheless provide a point of reference for more detailed theoretical and experimental work. In other words, ideally a more complete picture of intrinsic rotation drive should still be able to account for such a global scaling. Indeed, theoretical efforts have suggested a possible mechanism involving the H-mode pedestal that might explain this scaling.[8,30] In particular, a model including the $E\times B$ shear present in the H-mode pedestal is able to effectively reproduce the intrinsic scaling.

Figure 2 shows a plot of the edge intrinsic torque (obtained by volume integrating the inferred intrinsic torque density profile, $T^{edge}_{intrinsic}=\int_{\rho=0.8}^{\rho=1.0}\eta_{intrinsic}dV$) versus the global parameter W/I_p. The data were obtained by performing NBI torque sweeps in DIII-D H-mode plasmas during independent scans of the injected power (ranging from 2.3 to 7.8 MW) and I_p (0.65–1.0 MA), using the transient rotation crossing technique, as described in the introduction to this section. The data were obtained using β_N feedback control, such that β_N (and similarly the stored energy) was held constant, while the torque was swept by varying the balance of co- and counter-NBI. No specific effort was made to keep density constant during these scans, which varied between 3 and 6×10^{19} m^{-3}. Of course, since we are investigating the torque, rather than the velocity, there is no specific reason to constrain the density. The data set also contains points with electron cyclotron heating (ECH), although all shots are predominantly NBI heated. In general, we find a good correlation between the intrinsic torque and W/I_p. Even though W/I_p provides a reasonable proxy for the intrinsic rotation drive, it is more instructive to instead look at a more physical local quantity.

If $E\times B$ shear is the important quantity for intrinsic rotation drive in the edge, then we should be able to see a similar correlation between the edge intrinsic torque and the edge E_r shear. In cases such as presented here, where the toroidal rotation is nominally zero, E_r comes predominantly from the diamagnetic contribution to radial force balance, i.e., $E_r\sim\nabla P/Zen$, where Z is the ion charge and n is the ion density. A plot of the edge torque against the maximum of the edge pressure gradient is shown in Fig. 3(a). Indeed, a good correlation is found between the two quantities with a linear correlation coefficient of 0.8 (curiously, the correlation is somewhat worse with $\nabla P/n$). From this data set, one can obtain a simple expression for the edge intrinsic torque (in N m) in terms of the edge pressure gradient for DIII-D plasmas,

$$T^{edge}_{intrinsic}=(0.255\pm0.081)-(2.79\pm0.46)\times10^{-3}\nabla P, \quad (5)$$

with ∇P (given in kPa/m) generally negative, resulting in a positive contribution to the torque. Interestingly, one notices that there remains (outside of error bars) a finite edge torque even in the absence of a pressure gradient. This may be indicative of a poloidal rotation contribution to radial force balance, which might be expected to be more significant in the pedestal with strong gradients.[31,32]

Of course, strictly speaking, the shear in E_r depends on the second derivative of the pressure, which is experimentally problematic to determine with high certainty. Nonetheless, for this data set, the profiles have been fitted with cubic

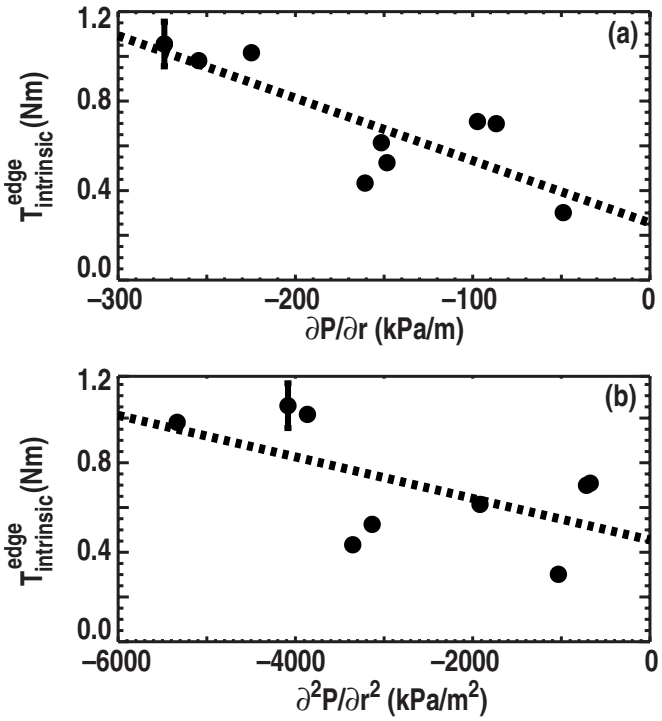

FIG. 3. (a) Plot of edge intrinsic torque vs edge pressure gradient showing strong correlation between these two local quantities. (b) A similar correlation is observed between the edge intrinsic torque and the second derivative of the pressure.

splines, and the second derivative estimated from the fits is shown for completeness in Fig. 3(b). Clearly the same underlying trend remains in the data, although increased scatter associated with larger uncertainties in the second derivative is apparent.

If the edge pressure gradient is indeed the source of the residual stress in the pedestal, as suggested by theory and which seems supported by the present data, then the H-mode pedestal in principle provides a universal mechanism for driving rotation in the plasma edge. This would be an advantageous feature for future burning H-mode plasmas. On the other hand, a pressure gradient driven residual stress would result in a less favorable projection of the intrinsic rotation to ITER than global scalings like W/I_p might suggest.[25] Specifically, a ∇P drive of intrinsic rotation is limited due to peeling-ballooning stability in the edge. Moreover, rotation resulting from ∇P driven residual stress has a diamagnetic scaling (i.e., proportional to ρ^*).

B. Inward pinch of angular momentum as a means of providing rotation shear

Although at this stage it is not clear what the optimal rotation profile would be for burning plasma devices like ITER, it is likely that some amount of rotation shear in the core would be desirable. In that case, having an edge source alone might not be sufficient. In the case of purely diffusive transport, rotation drive at the edge from the residual stress will result in a flat rotation profile inside of the effective source. On the other hand, if the transport results in a pinch of angular momentum, then a peaked profile can be produced from this edge source. Hence, the investigation of momentum transport via pinch mechanisms may be a critical part of the intrinsic rotation picture.

Generally, in order to isolate the role of the momentum pinch, one must modify the gradient in the toroidal velocity independently from the velocity, so as to avoid having collinearity in the angular momentum balance equation for the diffusive and pinch terms. Experimentally, a variety of techniques have been utilized to achieve this, for example, neutral beam perturbations and the braking torque from NRMFs.[13,18,33] The diffusive and pinch contributions to the transport are then determined by modeling the TAM flow through each radius, $M(\rho)=\int_0^\rho \Pi_\phi(\rho)dV$ (in N m), which is known experimentally from the measured rotation data and calculated beam source from TRANSP. Since the relaxation of the rotation profile is modeled only from the time the perturbation is turned off, the technique has the advantage that no specific knowledge of the perturbing source or its localization is required. We use a nonlinear least-squares fitter to solve for the time-independent χ_ϕ and V_{pinch} that best reproduce the time history of the TAM flow profile, as described in Refs. 13 and 18. Note that this analysis neglects the residual stress term. This is mostly a practical consideration, since additional degrees of freedom do not appear necessary to reproduce the TAM flow.

There have been theoretical descriptions for a pinch of angular momentum through low-k turbulence effects.[5,6] Favorable comparisons have been observed between these theories and experiment.[13,18,33] Theory has recently claimed a relatively weak dependence of the pinch on collisionality;[34] on the other hand, it has also been shown that a strong correlation exists between the collisionality and R/L_n (Ref. 35) (which *does* affect the momentum pinch both theoretically and experimentally). Hence, recent work on DIII-D and National Spherical Torus Experiment (NSTX) (Ref. 36) have been motivated to investigate the dependence of the pinch on collisionality.

In both devices, the collisionality was varied while trying to maintain other dimensionless quantities as close to constant as possible. This was done by changing the power (and hence temperature) at fixed density. This increases both β_N and ρ^*, both of which can be corrected by adjusting B^2 accordingly, and then similarly I_p^2 to keep q constant. The NSTX data come from H-mode plasmas, where 50 ms pulses of $n=3$ NRMFs were applied, and the resultant relaxation of the rotation after the NRMF was turned off was modeled to extract χ_ϕ and V_{pinch}. These plasmas had line average densities in the range $\bar{n}_e \sim 5.2 \pm 1.1 \times 10^{19}$ m^{-3} and $q_{95} \sim 10 \pm 0.5$, and as part of the collisionality scan, the toroidal field was varied between 0.35 and 0.55 T, and injected NBI power from 2.0 to 5.8 MW. The extracted pinch velocities variation with electron collisionality ν^* is shown in Fig. 4(a), collecting data between $0.5<\rho<0.8$. In general, the pinch velocity is found to decrease as the collisionality is reduced. Interestingly, there appears to be a second branch of data points at higher (inward) pinch velocity for the same collisionality, but the reason for this is not yet understood.

Also shown on the same plot is a data set obtained from DIII-D L-mode plasmas. In these plasmas, the rotation was

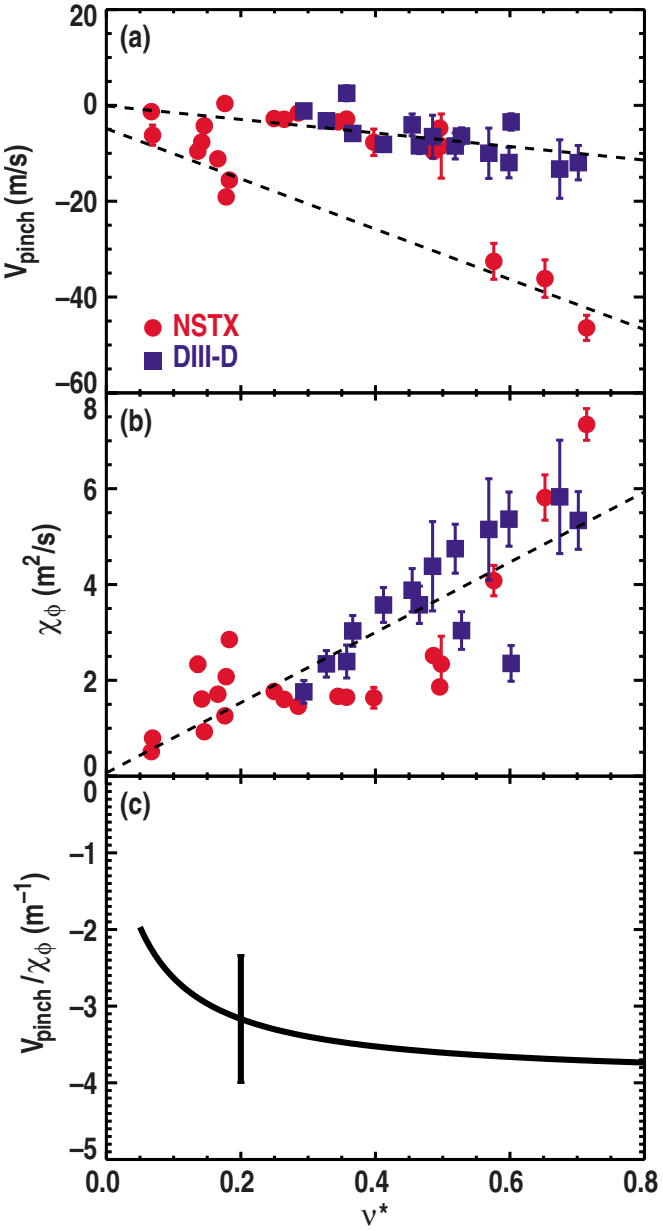

FIG. 4. (Color online) (a) Pinch velocity V_{pinch}, (b) momentum diffusivity χ_ϕ, and (c) pinch ratio V_{pinch}/χ_ϕ vs local electron collisionality ν^*. There appears to be only a weak dependence of the pinch ratio on collisionality.

modified using torque modulations from the neutral beams at constant power (by varying the balance of co- and counter-beams). These plasmas ran with $\bar{n}_e \sim 2.5 \pm 0.1 \times 10^{19}$ m^{-3} and $q_{95} \sim 4.9 \pm 0.5$, and the power was varied between 1.9 and 5.3 MW with the field scanned between 1.3 and 2.1 T. The data shown are obtained from the radial region $0.25 < \rho < 0.85$. Although there is a strong overlap between the data sets from the two devices, this is presumably just fortuitous, since no explicit attempt was made to match the experiments. Indeed, the difference in q_{95} might be expected to slightly modify the pinch based on simulations in Ref. 34. Nonetheless, the same trend is manifested in the DIII-D data with a clear reduction in the pinch velocity with collisionality. Hence, the data suggest that there is some commonality in the physics mechanisms responsible for the momentum pinch at both low and conventional aspect ratios.

In terms of peaking the rotation profile, the relative ratio of the pinch to the momentum diffusivity is more important than the absolute pinch velocity. The inferred momentum diffusivities for both machines are plotted in Fig. 4(b). These data too show a strong dependence on collisionality. One complication is the fact that although the experiments were conducted as collisionality scans, R/L_n was found to vary significantly in this data set. To deal with this, we have performed a multiple regression on the V_{pinch} and χ_ϕ versus both ν^* and R/L_n. The regression analysis finds that $\chi_\phi = (6.09 \pm 0.72)\nu^* + (0.157 \pm 0.072)R/L_n$ and $V_{pinch} = (-24.2 \pm 3.5)\nu^*$. Note that while χ_ϕ is found to depend on both variables, the p-values for R/L_n and ν^* suggest that one parameter can be neglected for V_{pinch}. Individual linear fits between V_{pinch} and these parameters indicate a higher correlation between V_{pinch} and ν^*. From these expressions, we can plot the pinch ratio V_{pinch}/χ_ϕ as a function of ν^*, as shown in Fig. 4(c), for a typical $R/L_n = 2$. This shows a very weak dependence of the pinch ratio on collisionality. It should be noted that in this data set, ν^* and R/L_n are correlated with a correlation coefficient of approximately 0.7. Therefore, an entirely flat V_{pinch}/χ_ϕ cannot be ruled out. In any case, it remains feasible that the intrinsic rotation profile might be peaked in future devices such as ITER (where the collisionality can be expected to be in the range $0.05 < \nu^* < 0.1$), originating from an effective edge torque, coupled with an inward pinch of angular momentum in the core.

C. Residual stress in the core

In principle, residual stress mechanisms may be active in the core of the plasma as well. Generally, $E \times B$ shear is likely to be smaller, although plasmas with strong internal transport barriers may still allow this to play a role. As such, we may expect other documented effects, such as up-down asymmetries[9] or charge separation,[10] to play a relatively more important role in intrinsic rotation drive in the core.

We return to the data set presented in Sec. II A and now focus on the effective torque in the core, obtained by integrating the intrinsic torque density from the plasma center out to midradius, $T_{intrinsic}^{core} = \int_{\rho=0}^{\rho=0.5} \eta_{intrinsic} dV$. A similar plot to that presented in Fig. 3 but substituting the peak edge pressure gradient with the equivalent quantity in the core is shown in Fig. 5. A number of key observations can be made. First, unlike at the edge, there does not appear to be any strong correlation between the local pressure gradient and the core intrinsic torque, suggesting that while $E \times B$ shear may explain the edge torque, it is likely not the dominant drive in the core. Second, the torque in the central region of the plasma tends to be relatively small compared with that at the edge. However, perhaps most significantly, there is a very clear outlier, showing a torque more comparable to that at the edge, but interestingly, in the counterdirection. This point turns out to have ECH power (~1.6 MW) deposited on axis. Even if configured for current drive (which was not the case here), the direct momentum input for ECH is about a factor

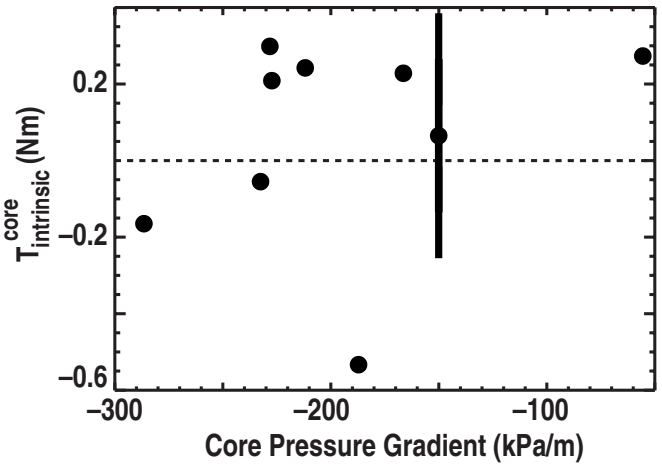

FIG. 5. Plot of core intrinsic torque (integrated between $0<\rho<0.5$) and the local core pressure gradient. Unlike at the edge, the core torques do not show a strong correlation with pressure gradient. The core torque tends to be smaller compared with the edge, although as illustrated by one data point, at least under some conditions, significant counterintrinsic torque can be driven in the core.

of 300 or so less than NBI for the same power, which here might amount to just 0.01 N m. Apparently then, the intrinsic drive in the core can be directly manipulated, in this case by means of ECH. The modifications result presumably through some change in the underlying profiles and turbulence, so the rotation may still be considered intrinsic (in the sense of being "intrinsic" to the plasma profiles), although the effect is through a different method than simple modification of the pressure gradient. Interestingly, ECH was also determined to modify the intrinsic rotation on JT-60U;[37] however, the effect was exactly the opposite than reported here for DIII-D, namely, with the ECH driving cointrinsic rotation. Electromagnetic waves have also been observed to modify the intrinsic rotation on C-Mod (Ref. 38) using lower hybrid current drive[39] and ion cyclotron frequency mode conversion,[40] and more recently, results from NSTX have suggested that high harmonic fast wave heating may also result in a countertorque in the core plasma, and perhaps also directly modifies even the edge torque.[41] This, of course, should only serve to reinforce the fact that there is much richer physics involved in the core intrinsic rotation drive, and suggests further work is required to properly characterize this.

One general problem with the experimental techniques outlined so far for determining the intrinsic torque is that they do no readily lend themselves to plasmas which are usually run with high rotation. Such plasmas that have not been fully optimized to low rotation include quiescent H modes (QH modes), advanced tokamak and hybrid plasmas. Nonetheless, it is obviously still desirable to understand what role, if any, the intrinsic rotation plays in these plasmas.

QH-mode plasmas are particularly interesting in the context of intrinsic rotation. Generally, QH-mode plasmas have been found to be more robust with rapid counter-rotation. To some extent, the existence of cocurrent intrinsic rotation drive tends to be counterproductive to QH-mode operation, since it would tend to oppose the NBI torque, resulting in a smaller rotation. However, there have been several indications that the intrinsic torque may be relatively weak in QH-mode plasmas. For example, QH modes have been run down below −1 N m of NBI torque, yet still rotate in the counterdirection. Following the simple estimates of the intrinsic torque, as described in this paper, would suggest intrinsic torques of 2 N m or more for these QH-mode plasmas. One might naively expect that the intrinsic torque would overwhelm the NBI torque, resulting in cocurrent directed rotation. Similarly, as shown in Ref. 42, the rotation profile from an edge localized mode (ELM)-free H mode, occurring after QH mode was lost when the rotation was driven too low, is found to be relatively small, again suggesting small overall intrinsic torque. One possible explanation would be that there is some mechanism responsible for large counterdriven intrinsic torques in the core of QH-mode plasmas, which balances the drive in the pedestal, resulting in the apparently small intrinsic torque.

To investigate this possibility, we have developed an alternate technique for estimating the intrinsic torque in plasmas with finite rotation. The concept is to use a transient NBI torque step, preferably a relatively small perturbation to minimize the changes to the background transport. For any assumed level of intrinsic torque, one can determine the momentum confinement time $\tau_\phi = L/(T_{\mathrm{NBI}}+T_{\mathrm{intrinsic}})$, where $L=\int nmRV_\phi dV$ is the total angular momentum, in the stationary part of the discharge. The momentum confinement time so determined should also properly describe the relaxation of the rotation immediately following the torque step. Hence, one can determine the level of intrinsic torque required to obtain a momentum confinement time that is consistent both during the steady and transient part of the discharge. To some extent, the intrinsic torque so-determined can be considered the "missing" torque required to make the steady state and transient momentum confinement times equal.

One complication is that the torque step and consequent change in the rotation tend to modify the confinement, as evident through changes in, say, the energy confinement time τ_E of 10%–20%. In other words, using a constant τ_ϕ over this evolution period is probably not completely justified. To try to deal with this better, we allow for a dynamic momentum confinement time using a linear mapping between the momentum confinement time and the energy confinement time based on the stationary time periods. We then use this time varying momentum confinement time to numerically solve for the angular momentum evolution during the time interval. Since the inferred time-varying momentum confinement time is still dependent on the assumed intrinsic torque, we can use a nonlinear least-squares fitter to solve for the intrinsic torque by finding the best match to the measured angular momentum time history.

We can take the analysis a step further and utilize a "shell-peeling" technique to infer the complete intrinsic torque profile. Specifically, one considers successively smaller plasma volumes in the 0D model, so $T_{\mathrm{intrinsic}}(\rho)$ is obtained by considering the angular momentum to that ρ, $L(\rho)=\int_0^\rho nmRV_\phi dV$. Of course, it is not *a priori* clear that this simple zero-dimensional (0D) model is able to adequately capture the physics represented in Eqs. (1) and (2). Therefore, we have benchmarked this technique in plasmas where

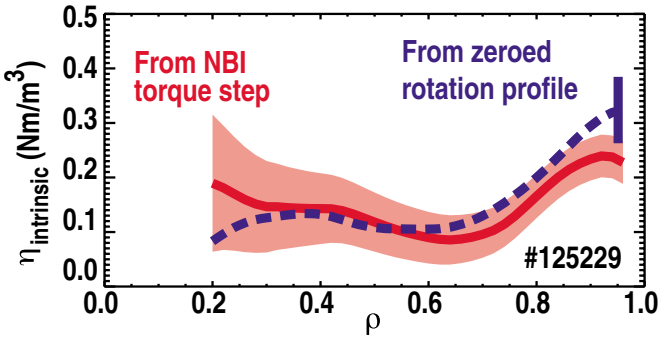

FIG. 6. (Color online) Comparison of different methods of extracting the intrinsic torque density profile. In one case, the torque is estimated from the amount of neutral beam torque required to bring the rotation profile to zero (dashed), and the other utilizes a technique whereby the neutral beam torque is stepped down to infer the missing intrinsic torque. The shaded region represents the uncertainty in extracting the intrinsic torque density using the second of these techniques.

the rotation profile was successfully brought to zero and find the torque obtained from this transient analysis to be quantitatively comparable. An example of this is shown in Fig. 6, comparing the intrinsic torque density profile obtained by the usual method of zeroing out the rotation profile with that found by using the aforementioned NBI torque stepping technique. Note that the error in the torque density becomes large as one approaches the axis due to the successively smaller volume element. However, the integrated intrinsic torque profile maintains an uncertainty below 0.1 N m.

This technique has been applied to a DIII-D QH-mode plasma with $T_i(0) \sim 6$ keV, $T_0(0) \sim 5$ keV, and relatively high line average density $\bar{n}_e \sim 4 \times 10^{19}$ m^{-3}. The NBI torque is initially -2.8 N m and the central toroidal velocity is -150 km/s. At 3.9 s into the discharge, the torque is stepped down to -2.0 N m, as shown in Fig. 7, and the velocity eventually slows to approximately -100 km/s. We use this step to estimate the intrinsic torque in this QH-mode plasma, following the technique just described. The result is shown in Fig. 8. We see the typical edge intrinsic torque common to all the H modes investigated. For this plasma, the edge pedestal is approximately -250 kPa/m, and Eq. (5) would give an expected edge torque of 0.95 ± 0.22 N m, comparable to the measurement here of approximately 0.8 N m, again obtained by integrating the torque between $0.8 < \rho < 1.0$. So, the QH-mode edge intrinsic drive behaves similarly to our other H modes. However, unlike our typical H mode, the QH-mode plasma indeed has a very large counterintrinsic torque, extending from the center to almost the pedestal. In fact, the two regions produce torques comparable in magnitude, resulting in a very small net intrinsic torque. Note that in this particular case, the core counterintrinsic torque exceeds the edge torque, and the net intrinsic torque is actually slightly counter.

Some preliminary investigations of residual stress in the core with the global gyrokinetic code GYRO (Ref. 12) have been initiated. Since both the TAM flow M and the ion (as well as electron) power flow P (megawatt) can vary manyfold by 10% level variations in the ion temperature gradient length, the simulations have compared the calculated M/P

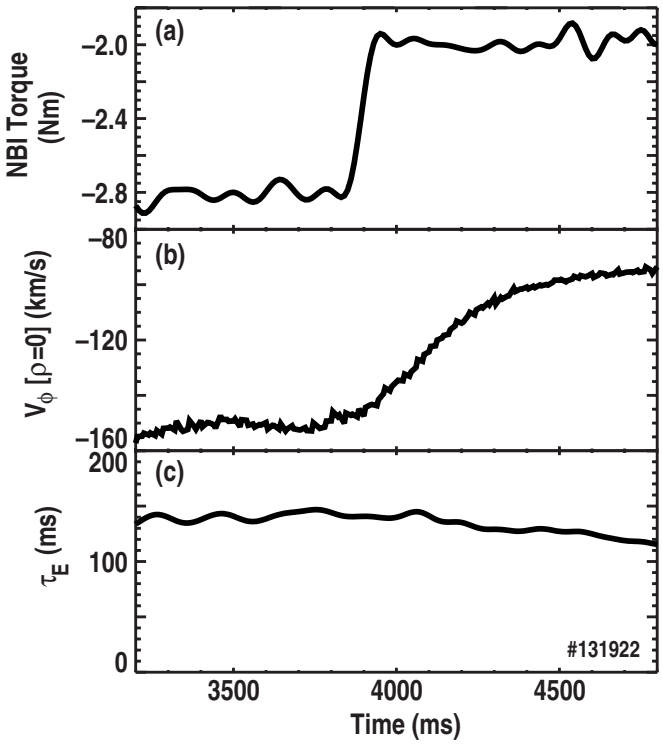

FIG. 7. (a) Neutral beam torque (as calculated by TRANSP), (b) central toroidal velocity, and (c) energy confinement time during preprogrammed torque step in a DIII-D QH-mode plasma.

radial profiles with the experimental profiles. In the residual stress shots, the small (within error bars) toroidal rotation and shear in toroidal rotation have a negligible effect on M/P in the simulation, compared with setting them identically to zero. The small diamagnetic $E \times B$ shear also makes only a very small contribution to M/P in the core. The effect of up-down asymmetry (using exact shaped geometry) was very weak and mostly at the outer radius. Most surprising was the novel result that a nonlocal or "profile variation" contribution to the residual stress can be quite large. From one particular profile data fit, the simulated M/P matched the (all positive) experimental M/P almost perfectly. However another profile data fit of the same discharge (with, for example, small 10% differences in the ion temperature gradient length profile), the M/P, did not agree well at all in (similar magnitude but flipping sign over the radial profile). Removing the profile variation (as well as the other symmetry breaking mechanisms) gave approximately zero M/P as required of the code test. If the extreme sensitivity of the residual stress to small changes in the profile variation continues to hold, it does not bode well for local gyro-Bohm transport models being able to treat low diamagnetic level TAM transport. For example, Kelvin–Helmholtz, toroidal Coriolis pinch, $E \times B$ shear, and up-down asymmetry have already been built into the latest version of TGLF,[43] but formulating the nonlocal profile variation contribution to residual stress will be very challenging.

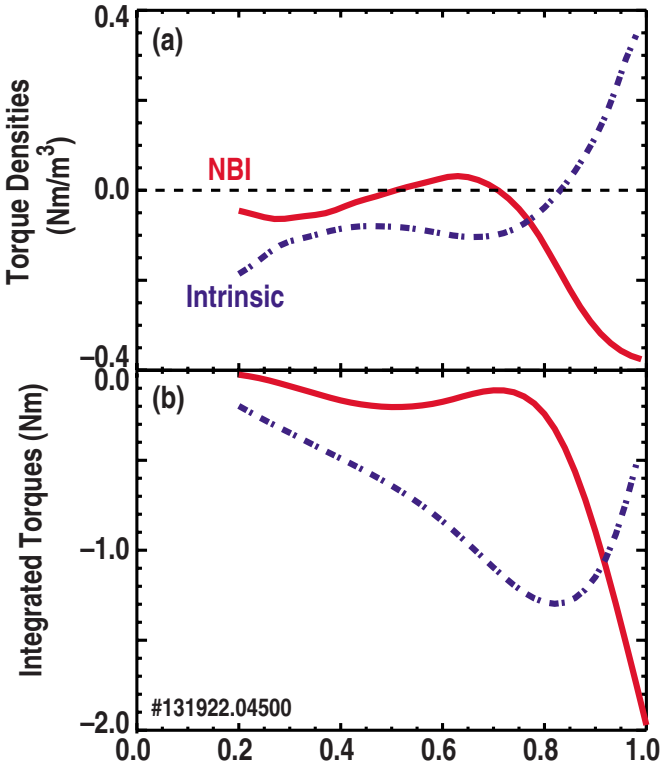

FIG. 8. (Color online) (a) Torque density and (b) integrated torque profiles from the neutral beams (solid) and the intrinsic source (dash-dot) for a DIII-D QH-mode plasma.

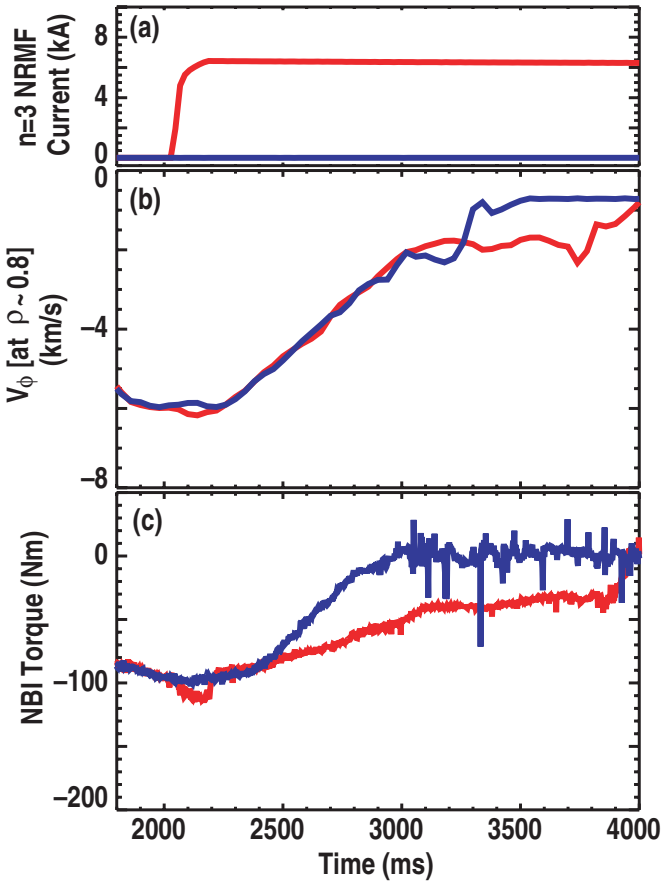

FIG. 9. (Color) Time histories of companion discharges with (red) and without (blue) $n=3$ NRMF: (a) $n=3$ coil current, (b) toroidal velocity near $\rho \sim 0.8$, and (c) NBI torque. For the same torque, the shot with the $n=3$ maintains a higher counter-rotation, owing to the countertorque from the NRMF.

III. ENHANCEMENT OF NRMF DRIVE AT LOW RADIAL ELECTRIC FIELD

As an alternative to relying on the intrinsic rotation, we also consider the possibility of driving the rotation externally without direct momentum injection. The radial flux of particles driven by NRMFs is dependent on collisionality regime. At typical finite radial electric field, as the collisionality is increased, one transitions from the so-called ν regime, where the transport goes as ν or $\sqrt{\nu}$ (Ref. 44) to the $1/\nu$ regime, so-named because the transport then exhibits a $1/\nu$-like dependence.[23] However, at low radial electric fields, other regimes, such as the superbanana plateau,[45] are also found to exist. In such regimes, the orbits of some particles effectively become unbounded, resulting in a significant enhancement in the transport and associated NRMF torque. Recent experiments at DIII-D have confirmed the existence of this peak in the NRMF torque.[46]

This enhanced NRMF torque at low rotation has been exploited to expand the operating space of QH-mode plasmas.[47] Since NRMFs add a countertorque to the plasma (at least when below the offset rotation), this is able to help maintain a higher counter-rotation for the same level of external counter-NBI torque, which is beneficial to QH-mode operation. In other words, the addition of NRMFs allows access to QH modes at lower levels of externally applied NBI torque. Favorably, the NRMF torque enhancement at low rotation further strengthens this effect by making it increasingly difficult for the rotation to slow down.

In Fig. 9, we have a pair of companion DIII-D shots with a NBI torque ramp, starting from large countertorque, reducing toward zero. In one of the shots, an $n=3$ NRMF is applied at $t=2000$ ms, prior to the NBI torque ramp. As expected, the rotation evolves very differently for the two shots. One can use such pairs of discharges to perform a complete analysis of both the NRMF torque and intrinsic torque.

Starting from the reference shot, with no NRMF, one can model the angular momentum evolution, again following a simple 0D model

$$\frac{\partial L}{\partial t} = T_{\mathrm{NBI}} + T_{\mathrm{intrinsic}} - \frac{L}{\tau_\phi}. \tag{6}$$

For a constant torque ramp, the neutral beam torque can be written simply as $T_{\mathrm{NBI}}=T_0+T_1 t$. Assuming the intrinsic torque does not change during the ramp, one can solve this analytically to obtain

$$L = (T_0 + T_{\mathrm{intrinsic}})\tau_\phi + T_1\tau_\phi t + T_1\tau_\phi^2(e^{-t/\tau_\phi} - 1). \tag{7}$$

The last term in Eq. (7) is an initial transient response, which becomes comparatively small compared with the second (linear) term after a few momentum confinement times. Hence, the intrinsic torque can be determined from the initial angular momentum (provided the external NBI torque is calculated), and the momentum confinement time is known from

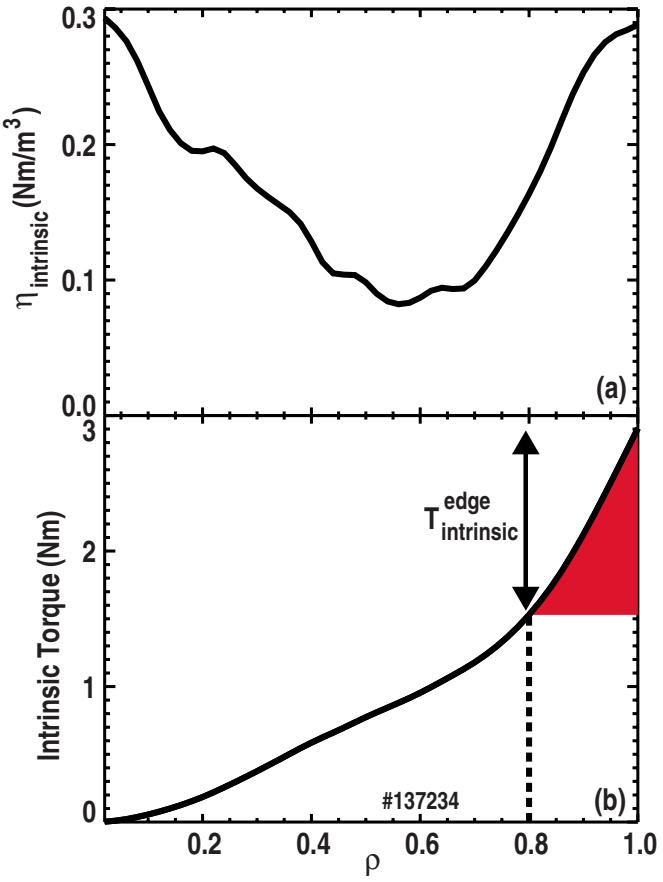

FIG. 10. (Color online) Profiles of (a) intrinsic torque density and (b) integrated intrinsic torque from reference shot with no $n=3$ NRMF in Fig. 9. The edge intrinsic torque is shaded.

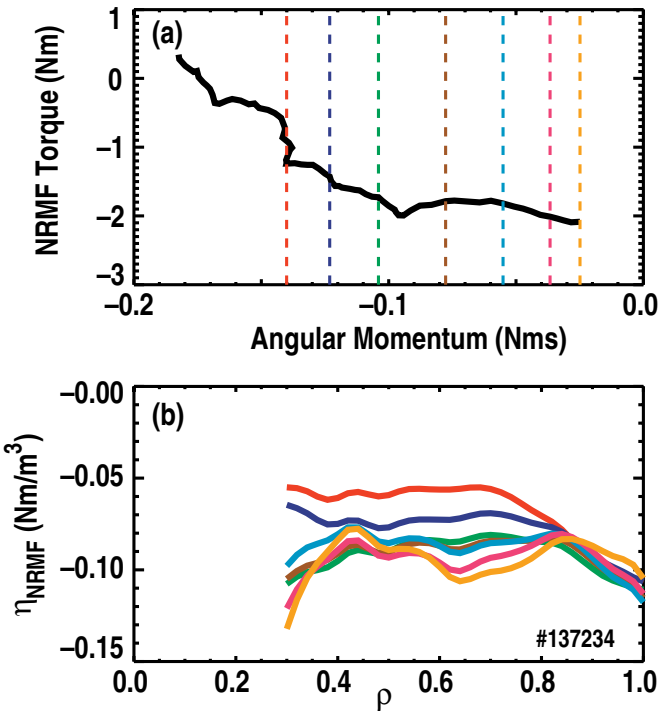

FIG. 11. (Color) (a) Evolution of the NRMF torque as the angular momentum is externally slowed by means of NBI. As the NBI drives the rotation toward zero, the NRMF torque becomes increasingly larger in magnitude (note negative), trying to restore the rotation toward the offset rotation (a corresponding "offset angular momentum" can be identified by the location where the NRMF torque is zero). (b) NRMF torque density profiles at the various times indicated in (a).

the slope of the angular momentum versus time curve for a given NBI torque ramp rate. Therefore, this reference discharge provides the key momentum transport characteristics of the plasma.

As before, we can use this model to uncover the local intrinsic torque profile using the shell-peeling technique discussed earlier in Sec. II C. This yields an intrinsic torque profile, as shown in Fig. 10, from which the intrinsic torque density profile can be readily backed out. Again, the intrinsic torque density profile has a peak in the pedestal region. If one extracts the edge torque from $\rho=0.8$ to $\rho=1$, as was discussed in Sec. II A, one finds a value of 1.38 N m. The edge pressure peaks at -360 kPa/m, which, if substituted into the expression relating the edge pressure to the edge intrinsic torque [Eq. (5)], one obtains an expected edge torque of 1.26 ± 0.25 N m, in good agreement with this analysis. Note that the total effective intrinsic torque for this plasma is approximately 2.9 N m, significantly different than the QH-mode plasma described in Fig. 8 (approximately -0.5 N m). This results from the very different core intrinsic torques. While it is not clear what causes this dramatic change, it is interesting to note that a key difference between the two plasmas is that the case with large countertorque in the core is a balanced double null shape, whereas the QH mode considered in this analysis is lower single null.

One can test whether the assumption of the intrinsic torque being a constant is valid during these torque ramps by subdividing the torque ramp into smaller time intervals and performing the same analysis on each window. We find that both the total intrinsic torque as well as the edge intrinsic torque decrease as the angular momentum is reduced, albeit very minimally (less than 5% variation from the beginning to the end of the ramp).

Now, we can compare the evolution of the angular momentum in the case with the NRMF applied. In that case, we must add another term to the right hand side of Eq. (6) to account for the NRMF torque, T_{NRMF}. Note that we do not consider the possibility that the neutral beam torque is modified due to anomalous fast ion losses associated with the NRMF; indeed previous measurements using a fast ion loss detector have not shown enhanced losses when the NRMF is on. We may immediately rearrange the equation to solve for the NRMF torque,

$$T_{NRMF} = \frac{\partial L}{\partial t} - T_{NBI} - T_{intrinsic} + \frac{L}{\tau_\phi}. \quad (8)$$

From the reference discharge, we have the time history evolution of the intrinsic torque (which practically we could choose to ignore, given the relatively small dependence on L). This evolution is shown in Fig. 11(a). One sees that the (counter)-NRMF torque increases as the angular momentum is reduced by external means, in this case from the NBI ramp. Unlike resonant braking, where the torque also increases as the rotation is slowed, in this case, of course, the

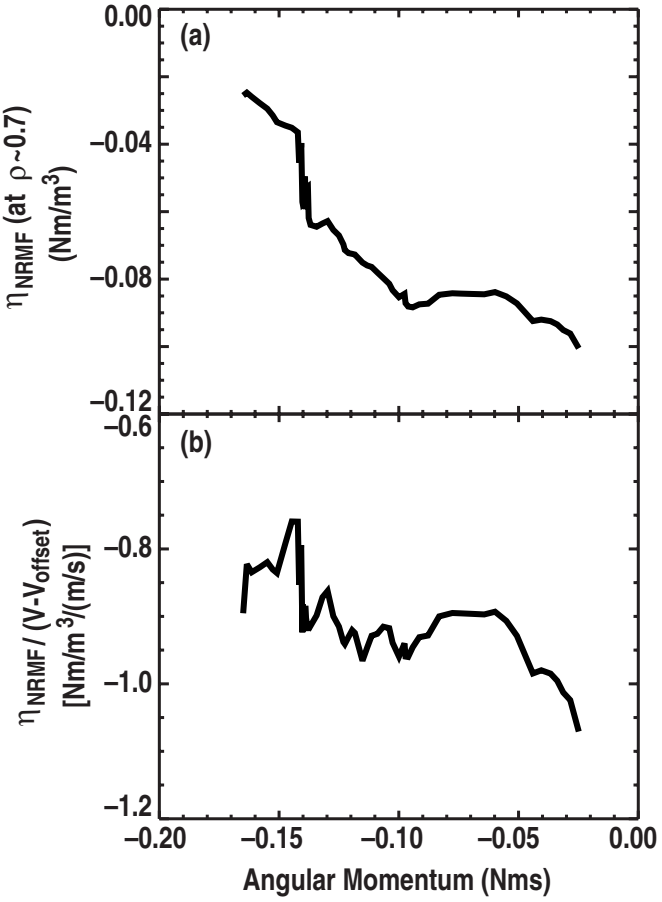

FIG. 12. (a) NRMF torque density at $\rho=0.7$ and (b) NRMF torque strength vs measured angular momentum varied externally by neutral beams. As low rotation the torque strength increases, qualitatively consistent with the idea of NRMF torque enhancement at low rotation.

torque is such as to try to accelerate the plasma rather than brake it. From a practical point of view, this means that if any phenomenon in the plasma tries to slow the plasma rotation (e.g., a magnetohydrodynamic mode), then the NRMF applies an increasingly large restoring torque, trying to maintain the rotation.

We can again peel back shells to recover the evolution of the NRMF torque profile. A sequence of such profiles is shown in Fig. 11(b) at select times in the angular momentum evolution [as indicated by the dashed lines in Fig. 11(a)]. One sees that the torque density is relatively broad as previously reported, and, consistent with the global picture from Fig. 11(a), is found to increase as the angular momentum is reduced. A local plot of the NRMF torque density at $\rho=0.7$ is shown in Fig. 12. Now, one should expect the torque to increase as we move away from the offset velocity due to the linear dependence on V_ϕ seen in Eq. (3). However, if we divide this out, we see that the NRMF strength k also increases as the velocity is reduced toward zero, qualitatively consistent with the picture of an enhancement of the NRMF torque at low rotation. In other words, in this region of velocity space (i.e., counter-rotation below the offset), both the proximity to the offset velocity and the NRMF strength reinforce each other to minimize further rotation slowing.

IV. SUMMARY OF RESULTS

We have focused on two possible mechanisms that might be exploited in future burning plasma devices to drive rotation without relying on direct injection of angular momentum from neutral beams. The generation of intrinsic rotation has been considered separately in the edge and core. In the edge, a fairly simple picture has emerged, showing in general a strong scaling with the intrinsic torque at the edge with the edge pressure gradient. This appears consistent with theories for residual stress in this region driven by strong $E\times B$ shear. A pinch of angular momentum looks suitable for taking this edge torque and producing sheared rotation profiles. While intrinsic rotation drive is also seen in the core, the physics responsible for it appears much more complicated, and no equivalent single parameter effect is observed.

The torque driven by NRMFs is clearly another important avenue to consider for driving rotation in future devices. This has many potentially beneficial features due to the offset rotation and enhancement at low rotation. As noted in Ref. 48, the offset rotation for ITER baseline operation is approximately 0.4% of the Alfvén velocity and may be sufficient to provide rotational stability for resistive wall modes and neoclassical tearing modes. Moreover, although NRMFs decrease the plasma's tolerance to error fields and mode locking for corotating plasmas,[49] more recent studies in counter-rotating plasmas suggest that NRMFs can actually improve the resilience to locked modes.[47] Therefore, if NRMF driven rotation is to be fully exploited in the future, then it will likely require operating with counter-rotation. This may provide additional incentive to further investigate and optimize QH-mode plasmas.

One complication is that these two torques compete with each other, since (at least at the edge) the intrinsic torque is cocurrent, whereas the NRMF torque is countercurrent (when starting from low rotation). Unfortunately, that can of course result in a situation where the two torques roughly cancel leaving no net torque. Indeed, in current DIII-D experiments, such as described in Sec. III, we have observed such situations.

The intrinsic error fields in a device like ITER are unlikely to be significant enough to drive large NRMF torques, so under such conditions, the intrinsic rotation drive is presumably most important. However, the application of resonant fields for ELM suppression may potentially result in very large NRMF torques, perhaps orders of magnitude larger than either the NBI or intrinsic torque.[48] Ultimately, it is reasonable to explore whether a combination of the effects might be exploited for rotation profile control.

ACKNOWLEDGMENTS

This work was supported in part by the U.S. Department of Energy under Grant Nos. DE-AC02-09CH11466, DE-FC02-04ER54698, DE-FG02-99ER54546, and DE-FG02-89ER53297.

[1] E. J. Strait, T. S. Taylor, A. D. Turnbull, J. R. Ferron, L. L. Lao, B. Rice, O. Sauter, S. J. Thompson, and D. Wróblewski, Phys. Rev. Lett. **74**, 2483 (1995).
[2] K. H. Burrell, Phys. Plasmas **4**, 1499 (1997).

[3]M. Shimada, D. J. Campbell, V. Mukhovatov, M. Fujiwara, N. Kirneva, K. Lackner, M. Nagami, V. D. Pustovitov, N. Uckan, J. Wesley, N. Asakura, A. E. Costley, A. J. H. Donn, E. J. Doyle, A. Fasoli, C. Gormezano, Y. Gribov, O. Gruber, T. C. Hender, W. Houlberg, S. Ide, Y. Kamada, A. Leonard, B. Lipschultz, A. Loarte, K. Miyamoto, V. Mukhovatov, T. H. Osborne, A. Polevoi, and A. C. C. Sips, Nucl. Fusion **47**, S1 (2007).
[4]J. D. Callen, A. J. Cole, and C. C. Hegna, Phys. Plasmas **16**, 082504 (2009).
[5]A. G. Peeters, C. Angioni, and D. Strintzi, Phys. Rev. Lett. **98**, 265003 (2007).
[6]T. S. Hahm, P. H. Diamond, Ö. D. Gürcan, and G. Rewoldt, Phys. Plasmas **14**, 072302 (2007).
[7]R. R. Dominguez and G. M. Staebler, Phys. Fluids B **5**, 3876 (1993).
[8]Ö. D. Gürcan, P. H. Diamond, T. S. Hahm, and R. Singh, Phys. Plasmas **14**, 042306 (2007).
[9]Y. Camenen, A. G. Peeters, C. Angioni, F. J. Casson, W. A. Hornsby, A. P. Snodin, and D. Strintzi, Phys. Rev. Lett. **102**, 125001 (2009).
[10]C. J. McDevitt, P. H. Diamond, Ö. D. Gürcan, and T. S. Hahm, Phys. Plasmas **16**, 052302 (2009).
[11]R. E. Waltz, G. M. Staebler, J. Candy, and F. L. Hinton, Phys. Plasmas **14**, 122507 (2007).
[12]J. Candy and R. E. Waltz, J. Comput. Phys. **186**, 545 (2003).
[13]W. M. Solomon, S. M. Kaye, R. E. Bell, B. P. LeBlanc, J. E. Menard, G. Rewoldt, W. Wang, and S. A. Sabbagh, Phys. Rev. Lett. **101**, 065004 (2008).
[14]M. Yoshida, Y. Koide, H. Takenaga, H. Urano, N. Oyama, K. Kamiya, Y. Sakamoto, G. Matsunaga, and Y. Kamada, Nucl. Fusion **47**, 856 (2007).
[15]T. Tala, K.-D. Zastrow, J. Ferreira, P. Mantica, V. Naulin, A. G. Peeters, G. Tardini, M. Brix, G. Corrigan, C. Giroud, and D. Strintzi, Phys. Rev. Lett. **102**, 075001 (2009).
[16]K. Ida, Y. Miura, T. Matsuda, K. Itoh, S. Hidekuma, and S.-I. Itoh, Phys. Rev. Lett. **74**, 1990 (1995).
[17]W. M. Solomon, K. H. Burrell, J. S. deGrassie, R. Budny, R. J. Groebner, J. E. Kinsey, G. J. Kramer, T. C. Luce, M. A. Makowski, D. Mikkelsen, R. Nazikian, C. C. Petty, P. A. Politzer, S. D. Scott, M. A. Van Zeeland, and M. C. Zarnstorff, Plasma Phys. Controlled Fusion **49**, B313 (2007).
[18]W. M. Solomon, K. H. Burrell, A. M. Garofalo, A. J. Cole, R. V. Budny, J. S. deGrassie, W. W. Heidbrink, G. L. Jackson, M. J. Lanctot, R. Nazikian, H. Reimerdes, E. J. Strait, and M. A. Van Zeeland, Nucl. Fusion **49**, 085005 (2009).
[19]E. Lazzaro, R. J. Buttery, T. C. Hender, P. Zanca, R. Fitzpatrick, M. Bigi, T. Bolzonella, R. Coelho, M. DeBenedetti, S. Nowak, O. Sauter, and M. Stamp, Phys. Plasmas **9**, 3906 (2002).
[20]W. Zhu, S. A. Sabbagh, R. E. Bell, J. M. Bialek, M. G. Bell, B. P. LeBlanc, S. M. Kaye, F. M. Levinton, J. E. Menard, K. C. Shaing, A. C. Sontag, and H. Yuh, Phys. Rev. Lett. **96**, 225002 (2006).
[21]A. M. Garofalo, K. H. Burrell, J. C. DeBoo, J. S. deGrassie, G. L. Jackson, M. J. Lanctot, H. Reimerdes, M. J. Schaffer, W. M. Solomon, and E. J. Strait, Phys. Rev. Lett. **101**, 195005 (2008).
[22]K. C. Shaing, S. P. Hirshman, and J. D. Callen, Phys. Fluids **29**, 521 (1986).
[23]K. C. Shaing, Phys. Plasmas **10**, 1443 (2003).
[24]A. Cole, C. Hegna, and J. Callen, Phys. Rev. Lett. **99**, 065001 (2007).
[25]J. E. Rice, A. Ince-Cushman, J. S. deGrassie, L.-G. Eriksson, Y. Sakamoto, A. Scarabosio, A. Bortolon, K. H. Burrell, B. P. Duval, C. Fenzi-Bonizec, M. J. Greenwald, R. J. Groebner, G. T. Hoang, Y. Koide, E. S. Marmar, A. Pochelon, and Y. Podpaly, Nucl. Fusion **47**, 1618 (2007).
[26]J. L. Luxon, Nucl. Fusion **42**, 614 (2002).
[27]R. Hawryluk, *Physics of Plasmas Close to Thermonuclear Conditions* (CEC, Brussels, 1980), Vol. 1, p. 19.
[28]R. J. Goldston, D. C. McCune, H. H. Towner, S. L. Davis, R. J. Hawryluk, and G. L. Schmidt, J. Comput. Phys. **43**, 61 (1981).
[29]A. Pankin, Comput. Phys. Commun. **159**, 157 (2004).
[30]P. H. Diamond, C. J. McDevitt, Ö. D. Gürcan, T. S. Hahm, W. X. Wang, E. S. Yoon, I. Holod, Z. Lin, V. Naulin, and R. Singh, Nucl. Fusion **49**, 045002 (2009).
[31]R. J. Groebner, K. H. Burrell, and R. P. Seraydarian, Phys. Rev. Lett. **64**, 3015 (1990).
[32]F. L. Hinton and Y.-B. Kim, Phys. Plasmas **2**, 159 (1995).
[33]S. M. Kaye, W. Solomon, R. E. Bell, B. P. LeBlanc, F. Levinton, J. Menard, G. Rewoldt, S. Sabbagh, W. Wang, and H. Yuh, Nucl. Fusion **49**, 045010 (2009).
[34]A. G. Peeters, C. Angioni, Y. Camenen, F. J. Casson, W. A. Hornsby, A. P. Snodin, and D. Strintzi, Phys. Plasmas **16**, 062311 (2009).
[35]M. Maslov, C. Angioni, and H. Weisen, Nucl. Fusion **49**, 075037 (2009).
[36]M. Ono, S. M. Kaye, Y.-K. M. Peng, G. Barnes, W. Blanchard, M. D. Carter, J. Chrzanowski, L. Dudek, R. Ewig, D. Gates, R. E. Hatcher, T. Jarboe, S. C. Jardin, D. Johnson, R. Kaita, M. Kalish, C. E. Kessel, H. W. Kugel, R. Maingi, R. Majeski, J. Manickam, B. McCormack, J. Menard, D. Mueller, B. A. Nelson, B. E. Nelson, C. Neumeyer, G. Oliaro, F. Paoletti, R. Parsells, E. Perry, N. Pomphrey, S. Ramakrishnan, R. Raman, G. Rewoldt, J. Robinson, A. L. Roquemore, P. Ryan, S. Sabbagh, D. Swain, E. J. Synakowski, M. Viola, M. Williams, J. R. Wilson, and NSTX Team, Nucl. Fusion **40**, 557 (2000).
[37]M. Yoshida, Y. Sakamoto, H. Takenaga, S. Ide, N. Oyama, T. Kobayashi, and Y. Kamada, Phys. Rev. Lett. **103**, 065003 (2009).
[38]H. Hutchinson, R. Boivin, F. Bombardia, P. Bonoli, S. Fairfax, C. Fiore, J. Goetz, S. Golovato, R. Granetz, M. Greenwald, S. Hubbard, J. Irby, B. LaBombard, B. Lipschultz, E. Marmar, G. McCracken, M. Porkolab, J. Rice, J. Snipes, Y. Takase, J. Terry, S. Wolfe, C. Christensen, D. Garnier, M. Graf, T. Hsu, T. Luke, M. May, A. Nemczewski, G. Tinio, J. Schachter, and J. Urbahn, Phys. Plasmas **1**, 1511 (1994).
[39]J. E. Rice, A. C. Ince-Cushman, P. T. Bonoli, M. J. Greenwald, J. W. Hughes, R. R. Parker, M. L. Reinke, G. M. Wallace, C. L. Fiore, R. S. Granetz, A. E. Hubbard, J. H. Irby, E. S. Marmar, S. Shiraiwa, S. M. Wolfe, S. J. Wukitch, M. Bitter, K. Hill, and J. R. Wilson, Nucl. Fusion **49**, 025004 (2009).
[40]Y. Lin, J. E. Rice, S. J. Wukitch, M. J. Greenwald, A. E. Hubbard, A. Ince-Cushman, L. Lin, M. Porkolab, M. L. Reinke, and N. Tsujii, Phys. Rev. Lett. **101**, 235002 (2008).
[41]J. C. Hosea and NSTX Team, Proceedings of the 18th Topical Conference on RF Power in Plasmas, Gent, Belgium, June 2009.
[42]K. H. Burrell, T. H. Osborne, P. B. Snyder, W. P. West, M. E. Fenstermacher, R. J. Groebner, P. Gohil, A. W. Leonard, and W. M. Solomon, Phys. Rev. Lett. **102**, 155003 (2009).
[43]G. M. Staebler, J. E. Kinsey, and R. E. Waltz, Bull. Am. Phys. Soc. **54**, 269 (2009).
[44]K. C. Shaing, P. Cahyna, M. Becoulet, J.-K. Park, S. A. Sabbagh, and M. S. Chu, Phys. Plasmas **15**, 082506 (2008).
[45]K. C. Shaing, S. A. Sabbagh, and M. S. Chu, Plasma Phys. Controlled Fusion **51**, 035009 (2009).
[46]A. J. Cole, J. D. Callen, C. C. Hegna, A. M. Garofalo, H. Reimerdes, W. M. Solomon, and DIII-D Team, "Observation of peak neoclassical toroidal viscous force in the DIII-D tokamak" (unpublished).
[47]A. M. Garofalo, K. H. Burrell, H. Reimerdes, W. M. Solomon, M. J. Lanctot, T. H. Osborne, and L. Schmitz, "Quiescent H-mode in tokamak plasmas with torque driven by static non-axisymmetric fields" (unpublished).
[48]A. M. Garofalo, W. M. Solomon, M. Lanctot, K. H. Burrell, J. C. DeBoo, J. S. deGrassie, G. L. Jackson, J.-K. Park, H. Reimerdes, M. J. Schaffer, and E. J. Strait, Phys. Plasmas **16**, 056119 (2009).
[49]H. Reimerdes, A. M. Garofalo, E. J. Strait, R. J. Buttery, M. S. Chu, Y. In, G. L. Jackson, R. J. La Haye, M. J. Lanctot, Y. Q. Liu, M. Okabayashi, J.-K. Park, M. J. Schaffer, and W. M. Solomon, Nucl. Fusion **49**, 115001 (2009).